NASA Contractor Report 182084
ICASE Report No. 90–56

ICASE

NUMERICAL METHODS FOR SYSTEMS OF CONSERVATION LAWS OF MIXED TYPE USING FLUX SPLITTING

Chi-Wang Shu

Contract No. NAS1–18605
August 1990

Institute for Computer Applications in Science and Engineering
NASA Langley Research Center
Hampton, Virginia 23665–5225

Operated by the Universities Space Research Association

National Aeronautics and
Space Administration

Langley Research Center
Hampton, Virginia 23665-5225

NUMERICAL METHODS FOR SYSTEMS OF CONSERVATION LAWS OF MIXED TYPE USING FLUX SPLITTING

Chi-Wang Shu [1]
Division of Applied Mathematics
Brown University
Providence, RI 02912

ABSTRACT

The essentially non-oscillatory (ENO) finite difference scheme is applied to systems of conservation laws $\mathbf{u}_t + \mathbf{f}(\mathbf{u})_x = 0$ of mixed hyperbolic-elliptic type. A flux splitting $\mathbf{f}(\mathbf{u}) = \mathbf{f}^+(\mathbf{u}) + \mathbf{f}^-(\mathbf{u})$, with the corresponding Jacobi matrices $\frac{\partial \mathbf{f}^\pm(\mathbf{u})}{\partial \mathbf{u}}$ having real and positive/negative eigenvalues, is used. The hyperbolic ENO operator is applied separately on $\mathbf{f}^+(\mathbf{u})_x$ and on $\mathbf{f}^-(\mathbf{u})_x$. The scheme is numerically tested on the van der Waals equation in fluid dynamics. We observe convergence with good resolution to weak solutions for various Riemann problems, which are then numerically checked to be admissible as the viscosity-capillarity limits. We also observe the interesting phenomena of the shrinking of elliptic regions if they are present in the initial conditions.

[1]Research was supported by the National Aeronautics and Space Administration under NASA Contract No. NAS1-18605 while the author was in residence at the Institute for Computer Applications in Science and Engineering (ICASE), NASA Langley Research Center, Hampton, VA 23665. Research also was partially supported by NSF Grant DMS-88-10150, NASA Langley Grant NAG-1-1145 and AFOSR Grant 90-0093.

1 Introduction

The system of conservation laws

$$\begin{cases} \mathbf{u}_t + \mathbf{f}(\mathbf{u})_x = 0 \\ \mathbf{u}(x,0) = \mathbf{u}^0(x) \end{cases} \tag{1.1}$$

is hyperbolic if the Jacobi matrix $\frac{\partial \mathbf{f}(\mathbf{u})}{\partial \mathbf{u}}$ has real eigenvalues and a complete set of eigenvectors. In recent years there have been a lot of activity in designing stable and accurate numerical methods for solving systems of hyperbolic conservation laws. The ENO (essentially non-oscillatory) high order finite difference method, [5], [6], [12], [13], is one of the successful approaches. The philosophy of ENO schemes is to use upwinding and adaptive stencils, based on the local "wind" direction (the sign of the relevant eigenvalue) and the local smoothness, in each of the local characteristic fields. ENO schemes can resolve the interactions of shocks and waves and complicated wave structures quite well, according to the numerical examples for the hyperbolic Euler equations of a polytropic gas in [6], [13]. ENO schemes are formally high order accurate, measured by local truncation errors. In some cases the actual order of accuracy may degenerate due to the frequent switching of stencils in the linearly unstable regions [9], [14]. There is a simple modification of ENO schemes, with no additional computational cost, [14], which overcomes this accuracy degeneracy problem. However, our experience seems to show that the original ENO scheme has very good resolution for nonlinear systems [13], [14], suggesting that the modification may not be necessary in such cases.

If the Jacobi matrix $\frac{\partial \mathbf{f}(\mathbf{u})}{\partial \mathbf{u}}$ in (1.1) has complex eigenvalues, the system becomes elliptic. The initial value problem (1.1) may not be well posed in the elliptic regions. However, in applications, (1.1) may still be of mixed hyperbolic-elliptic type. Examples include equations in fluid dynamics [17], elasticity [8] and the partial differential equations related to Lorenz systems [7], just to name a few. In this paper we use the van der Waals equation in fluid dynamics

$$\begin{cases} v_t + p(w)_x = 0, & w_t - v_x = 0 \\ v(x,0) = v^0(x), & w(x,0) = w^0(x) \end{cases} \tag{1.2}$$

with

$$p(w) = \frac{RT}{w-b} - \frac{a}{w^2} \tag{1.3}$$

where R, T, a, b are all positive constants, for our numerical examples. See, for example, [17] for details. Equation (1.2) corresponds to (1.1) with $\mathbf{u} = (v,w)^T$, $\mathbf{f}(\mathbf{u}) = (p(w), -v)^T$. The

two eigenvalues of the Jacobi matrix $\frac{\partial \mathbf{f}(\mathbf{u})}{\partial \mathbf{u}}$ are $\pm\sqrt{-p'(w)}$. For an ideal gas, the pressure $p(w)$ is a decreasing function of w, resulting in a hyperbolic system (1.2). However, during the co-existence of gas and liquid, $p'(w)$ may become positive within an interval, as in the case (1.3) with suitable parameters (Figure 1), making the system (1.2) elliptic in this region. The mathematical ill-posedness of the system in the elliptic region reveals the physical fact that the state in the elliptic region is not stable, and it typically evolves into "phase transitions", i.e., jumps across the elliptic regions in the weak solution. As in the hyperbolic case, there can be more than one weak solution, and there are efforts in the literature, e.g., [15],[16], [8], [2], [3], [10], [11], to establish admissibility criteria with the goal to single out one "physically relevant" weak solution. A weak solution $\mathbf{u} = (v, w)$ of (1.2) is called admissible as the viscosity-capillarity limits in [15] if it is the bounded a.e. limit of $\mathbf{u}^\epsilon = (v^\epsilon, w^\epsilon)$, satisfying

$$\begin{cases} v_t^\epsilon + p(w^\epsilon)_x = \epsilon v_{xx} - \epsilon^2 A w_{xxx}, \\ w_t^\epsilon - v_x^\epsilon = 0 \\ v^\epsilon(x,0) = v^0(x), \qquad w^\epsilon(x,0) = w^0(x) \end{cases} \tag{1.4}$$

as $\epsilon \to 0^+$. Here A is a positive constant, usually between 0 and $\frac{1}{4}$. The analysis usually starts with the Riemann problem

$$(v(x,0), w(x,0)) = \begin{cases} (v_L, w_L), & x < 0 \\ (v_R, w_R), & x > 0 \end{cases} \tag{1.5}$$

whose solutions contain most of the rich features (shocks, phase boundaries, rarefaction waves, etc.) for more general initial conditions. It is easier to consider each jump (shock, phase transition) separately, with a jump called locally admissible if it is the limit of the travelling wave solutions of (1.4). A weak solution is then called locally admissible if each of its jumps is locally admissible. Admissible or locally admissible solutions of the Riemann problems, e.g. [15],[10],[3], typically contain phase boundaries (discontinuities jumping across the elliptic regions) but do not achieve values inside the elliptic region. More general initial data is more difficult to analyse. It is interesting to know what happens if the initial condition contains elliptic regions. ¿From a computational point of view, if a shock capturing method, such as the ENO method in [6], [13] is to be used, discontinuities are typically spread out in two or three points, hence points can sit in elliptic regions even if the exact solution jumps across it.

One of the main ingredients of ENO schemes, and of many other non-oscillatory schemes such as TVD (total-variation-diminishing) schemes [4], is the approximation in each of the local characteristic fields. If the system becomes elliptic, local characteristic decomposition is no longer available. In Section 2 we propose a flux splitting $\mathbf{f}(\mathbf{u}) = \mathbf{f}^+(\mathbf{u}) + \mathbf{f}^-(\mathbf{u})$, with the corresponding Jacobi matrices $\frac{\partial \mathbf{f}^\pm(\mathbf{u})}{\partial \mathbf{u}}$ having real and positive/negative eigenvalues. This

is similar to the flux splitting used for hyperbolic systems, for example the Lax-Friedrichs splitting and the van Leer splitting [19]. The hyperbolic ENO operator is then applied separately on $\mathbf{f}^+(\mathbf{u})_x$ and on $\mathbf{f}^-(\mathbf{u})_x$, using the component version in the elliptic regions, since the characteristic decompositions of $\frac{\partial \mathbf{f}^\pm(\mathbf{u})}{\partial \mathbf{u}}$ have no physical meanings in such regions. This idea is described in the next section. In Section 3 we numerically test the scheme on the van der Waals equation (1.2)-(1.3). We observe convergence with good resolution to weak solutions for various Riemann problems. We then numerically check that these weak solutions are admissible as the viscosity-capillarity limits by computing (1.4) with a sequence of decreasing ϵ. We also compute the solution with smooth initial conditions, and observe the interesting phenomena of the shrinking of elliptic regions if they are present in the initial conditions.

2 The Numerical Scheme

We start with a flux splitting

$$\mathbf{f}(\mathbf{u}) = \mathbf{f}^+(\mathbf{u}) + \mathbf{f}^-(\mathbf{u}) \tag{2.1}$$

with the requirement that the Jacobi matrix $\frac{\partial \mathbf{f}^+(\mathbf{u})}{\partial \mathbf{u}}$ has only real and positive eigenvalues, and likewise that the Jacobi matrix $\frac{\partial \mathbf{f}^-(\mathbf{u})}{\partial \mathbf{u}}$ has only real and negative eigenvalues. If the system is hyperbolic, the simplest way to achieve such splitting is due to Lax-Friedrichs

$$\mathbf{f}^\pm(\mathbf{u}) = \frac{1}{2}(\mathbf{f}(\mathbf{u}) \pm \alpha \mathbf{u}), \qquad \alpha = \max_{i,\mathbf{u}} \mid \lambda_i(\mathbf{u}) \mid \tag{2.2}$$

where $\lambda_i(\mathbf{u})$ are the eigenvalues of the Jacobi matrix $\frac{\partial \mathbf{f}(\mathbf{u})}{\partial \mathbf{u}}$. For special classes of hyperbolic systems, such as the Euler equations of a polytropic gas, more sophiscated splittings with better physical meanings are available, e.g., van Leer's splitting [19]. For an elliptic system, the simple splitting (2.2) no longer works. In fact, any splitting with the Jacobi matrices $\frac{\partial \mathbf{f}^+(\mathbf{u})}{\partial \mathbf{u}}$ and $\frac{\partial \mathbf{f}^-(\mathbf{u})}{\partial \mathbf{u}}$ commuting with each other, as is the case in (2.2), will probably fail, because commuting matrices with distinct eigenvalues can be simultaneously diagonalized, hence the eigenvalues of their sum are simply the sum of their corresponding eigenvalues. However, a splitting similar to (2.2) with the scalar α replaced by a diagonal matrix:

$$\mathbf{f}^\pm(\mathbf{u}) = \frac{1}{2}(\mathbf{f}(\mathbf{u}) \pm \overline{\alpha}\mathbf{u}), \qquad \overline{\alpha} = \begin{pmatrix} \alpha_1 & & & \\ & \alpha_2 & & \\ & & \ddots & \\ & & & \alpha_m \end{pmatrix} \tag{2.3}$$

can usually yield a required splitting. For example, the flux $\mathbf{f}(\mathbf{u})$ in the van der Waals equation (1.2) can be split successfully using (2.3) with:

$$\alpha_2 = \max_w \left(max \left(0, \frac{\sqrt{M^2 - 4p'(w)} - M}{2} \right) \right), \qquad \alpha_1 = \alpha_2 + M \tag{2.4}$$

and

$$M = a \max_w \sqrt{\max(0, p'(w))}, \qquad a > 2 \tag{2.5}$$

The idea is to make an ansatz $\mathbf{g}(\mathbf{u}) = M(v, 0)^T$, then try to find the smallest possible M such that the Jacobi matrices $\frac{\partial(\mathbf{f}(\mathbf{u}) \pm \mathbf{g}(\mathbf{u}))}{\partial \mathbf{u}}$ both have real and distinct eigenvalues. This leads to M given by (2.5). Once this is done, it is easy to use the Lax-Friedrichs idea, i.e., to add and substract $\alpha \mathbf{u}$ with a suitable α, to accomplish the splitting.

Equipped with the splitting (2.1), one can then apply any successful hyperbolic approximation techniques separately to $\mathbf{f}^+(\mathbf{u})$ and $\mathbf{f}^-(\mathbf{u})$. The only exception is that characteristic decompositions should not be performed in elliptic regions, since the characteristic directions of $\frac{\partial \mathbf{f}^+(\mathbf{u})}{\partial \mathbf{u}}$ and $\frac{\partial \mathbf{f}^-(\mathbf{u})}{\partial \mathbf{u}}$ do not have any physical meaning. In this paper we apply the ENO techniques developped in [12], [13] to $\mathbf{f}^+(\mathbf{u})$ and $\mathbf{f}^-(\mathbf{u})$.

We summarize the algorithm briefly in the following. More details can be found in [12], [13].

(1) The spatial operator

$$-\mathbf{f}(\mathbf{u})_x = -\mathbf{f}^+(\mathbf{u})_x - \mathbf{f}^-(\mathbf{u})_x \tag{2.6}$$

is approximated by a conservative flux difference

$$\begin{aligned} \mathbf{L}(\mathbf{u})_j &= \mathbf{L}^+(\mathbf{u})_j + \mathbf{L}^-(\mathbf{u})_j \\ &= -\tfrac{1}{\Delta x}(\hat{\mathbf{f}}^+_{j+\frac{1}{2}} - \hat{\mathbf{f}}^+_{j-\frac{1}{2}}) - \tfrac{1}{\Delta x}(\hat{\mathbf{f}}^-_{j+\frac{1}{2}} - \hat{\mathbf{f}}^-_{j-\frac{1}{2}}) \end{aligned} \tag{2.7}$$

where j is the grid index (the grids are located at $x_j = j\Delta x$), and the resulting ODE

$$\frac{\partial \mathbf{u}_j}{\partial t} = \mathbf{L}(\mathbf{u})_j \tag{2.8}$$

is discretized in the time variable t by a class of TVD (total-variation-diminishing) Runge-Kutta type high order methods introduced in [12]. For example, the third order case is

$$\begin{cases} \mathbf{u}^{(1)} = \mathbf{u}^{(0)} + \Delta t \mathbf{L}(\mathbf{u}^{(0)}) \\ \mathbf{u}^{(2)} = \frac{3}{4}\mathbf{u}^{(0)} + \frac{1}{4}\mathbf{u}^{(1)} + \frac{1}{4}\Delta t \mathbf{L}(\mathbf{u}^{(1)}) \\ \mathbf{u}^{(3)} = \frac{1}{3}\mathbf{u}^{(0)} + \frac{2}{3}\mathbf{u}^{(2)} + \frac{2}{3}\Delta t \mathbf{L}(\mathbf{u}^{(2)}) \\ \mathbf{u}^{(0)} = \mathbf{u}^n, \qquad \mathbf{u}^{n+1} = \mathbf{u}^{(3)} \end{cases} \tag{2.9}$$

In the following we will discuss the spatial operator $\mathbf{L}(\mathbf{u})_j$ in (2.7) and suppress the time variable t;

(2) The numerical fluxes $\hat{\mathbf{f}}^{\pm}_{j\pm\frac{1}{2}}$ in (2.7) approximate $\mathbf{h}^{\pm}(x_{j\pm\frac{1}{2}})$ to high order, where the functions $\mathbf{h}^{\pm}(x)$ are defined implicitly by

$$\mathbf{f}^{\pm}(\mathbf{u}(x)) = \frac{1}{\Delta x}\int_{x-\frac{\Delta x}{2}}^{x+\frac{\Delta x}{2}} \mathbf{h}^{\pm}(\xi)d\xi \tag{2.10}$$

see [13] for the derivation. r-th order polynomial interpolation is used, based on Newton differences. The approximation to $\mathbf{h}^{\pm}(x)$ is carried out component by component. In the following we will use plain letters to represent one component of the corresponding vector in bold letters, and we will suppress the superscripts $\pm$. As is pointed out in [13], there is no need to construct the function $h(x)$ or its Newton differences explicitly: one can simply use the difference tables of $f(u(x))$. If the undivided differences of $f(u(x))$ are computed by

$$\begin{aligned} f[j,0] &= f(u_j) \\ f[j,k] &= f[j+1,k-1] - f[j,k-1], \qquad k = 1,...,r \end{aligned} \tag{2.11}$$

where r is the order of the interpolation polynomial, then the numerical flux $\hat{f}_{j+\frac{1}{2}}$ is obtained by

$$\hat{f}_{j+\frac{1}{2}} = \sum_{k=0}^{r} C(i-j,k)f[i,k] \tag{2.12}$$

where i is the left-most point in the stencil used to approximate $\hat{f}_{j+\frac{1}{2}}$, and $C(s,k)$ is defined by

$$C(s,k) = \frac{1}{(k+1)!}\sum_{l=s}^{s+k}\prod_{\substack{p=s \\ p\neq l}}^{s+k}(-p) \tag{2.13}$$

The small matrix C is independent of the flux, hence can be computed only once and then stored. The reader can easily check that (2.12)-(2.13) gives the correct interpolant approximation to the function $h(x)$.

What distinguishes ENO from other finite difference methods is the adaptive stencil idea. This idea is realized through the choice of i, the left-most point in the stencil used to approximate $\hat{f}_{j+\frac{1}{2}}$. We start with $i = j$ for computing $\hat{f}^{+}_{j+\frac{1}{2}}$ or $i = j+1$ for computing $\hat{f}^{-}_{j+\frac{1}{2}}$. This is due to upwinding, since the eigenvalues of $\frac{\partial \mathbf{f}^{+}(\mathbf{u})}{\partial \mathbf{u}}$ are all positive, hence the information for $\mathbf{f}^{+}(\mathbf{u})$ propagates to the right, likewise the information for $\mathbf{f}^{-}(\mathbf{u})$ propagates to the right. The stencil is then expanded point by point, according to the principle of choosing the smaller in absolute value of the two relevant differences:

$$if\ (abs(f[i,k]).gt.abs(f[i-1,k]))\ i = i-1 \tag{2.14}$$

for $k = 1, ..., r$.

A factor can be introduced in (2.14) to bias towards the choice of a linearly stable centered stencil [14]. This modification can enhance the accuracy in some cases but may cause some over-compression effects [14]. Since for nonlinear systems the original ENO scheme works well numerically [6], [13], we do not use this modification in this paper.

The scheme described above is uniformly high order in space and time, measured by local truncation error analysis.

Remark 2.1 Since the schemes described above are conservative, any converged solution will be a weak solution of (1.1). It is more difficult to show that the limit solutions are admissible. If we take r, the order of the interpolating polynomial, to be zero, and use the splitting (2.1)-(2.2) for a hyperbolic system, we recover the classical Lax-Friedrichs scheme. It is well known that the Lax-Friedrichs scheme can be rewritten as a centered scheme plus a dissipation term approximately equal to $\frac{1}{2}\alpha\Delta x\mathbf{u}_{xx}$. If we use the splitting of the form (2.3), we can still think about it as a centered scheme plus a dissipation term of the form $\frac{1}{2}\tilde{\alpha}\Delta x\mathbf{u}_{xx}$. It is then reasonable, cf. [16], [2], to expect that the scheme converges to the admissible weak solutions. Ample numerical tests should be performed to assess the convergence and admissability for higher order schemes. The numerical examples in Section 3 are preliminary results in this direction.

Remark 2.2 If some fractional step method (e.g. Strang [18]) is used on the splitting (2.1), we end up with a scheme of the form (see (2.7)):

$$\mathbf{u}^{n+1} = (\mathbf{I} + \Delta t\mathbf{L}^{+})(\mathbf{I}+\Delta t\mathbf{L}^{-})\mathbf{u}^{n} \tag{2.15}$$

(for the next time step the two operators may reverse order). For a linear or nonlinear problem with *smooth* solutions, it is very easy to choose stable operators $(\mathbf{I} + \Delta t\mathbf{L}^{\pm})$, due to the hyperbolicity of $\mathbf{f}^{\pm}(\mathbf{u})$ in (2.1). However, this does not necessarily mean that the scheme (2.15) is stable, since $(\mathbf{I} + \Delta t\mathbf{L}^{\pm})$ may not commute with each other and may not be simultaneously diagonalizable. If the operators satisfy the more restrictive condition

$$\|\mathbf{I} + \Delta t\mathbf{L}^{+}\| \leq 1 + O(\Delta t) \qquad \|\mathbf{I} + \Delta t\mathbf{L}^{-}\| \leq 1 + O(\Delta t) \tag{2.16}$$

for any consistent norm, the fractional step scheme (2.15) will be stable.

3 Numerical Examples

We use the van der Waals equation (1.2)-(1.3) with $RT = 1$, $a = 0.9$ and $b = 0.25$. The graph of the corresponding $p(w)$ is in Figure 1. The system is elliptic for $\alpha \leq w \leq \beta$, where $\alpha = 0.574912$ and $\beta = 1.036251$. The so-called Maxwell line BE in Figure 1, where the two shaded areas are equal, intersects the curve of $p(w)$ at $w = m = 0.494273$ and $w = M = 1.405065$. The horizontal lines AD and CF in Figure 1 yield $\gamma = 0.483100$ and $\delta = 1.918618$.

We use the third order, i.e. (2.9) and (2.12) with $r = 3$, ENO scheme, described in Section 2. If the computational cell is contained completely inside one of the hyperbolic regions $w \leq \alpha$ or $w \geq \beta$, we use characteristic decompositions (the ENO-LF algorithm described in [12], [13]). Otherwise the component by component approximation described in Section 2 is used. The splitting used is (2.3)-(2.5) with $a = 2.2$. The time step Δt is restricted by a CFL number 0.6, i.e. $\Delta t \leq 0.6(\rho(\frac{\partial \mathbf{f}^+(\mathbf{u})}{\partial \mathbf{u}}) + \rho(\frac{\partial \mathbf{f}^-(\mathbf{u})}{\partial \mathbf{u}}))\Delta x$ where $\rho(A)$ is the spectral radius of A.

All the computations are performed by using a sequence of refined meshes to verify convergence, although we typically only show the graphs for one or two fixed meshes.

We first compute several Riemann problems (1.5):

(1) $(v_L, w_L) = (1, m)$, $(v_R, w_R) = (1, M)$ where m and M are the Maxwell values defined above. This initial condition satisfies the Rankine-Hugoniot condition for a stationary jump. Physical principles (Maxwell equal area rule) and many admissibility criteria (e.g. the viscosity-capillarity criterion in [15], see (1.4)) indicate that this is an admissible jump. Our numerical result shows a stable, sharp jump for this case, Figure 2. We remark that here and in what follows, the numerical solution usually has one or two transition points in the elliptic region for the phase jump. Apparently they do not cause any trouble to the computation.

(2) $(v_L, w_L) = (1, 0.54)$, $(v_R, w_R) = (1, 0.54)$. This initial condition also satisfies the Rankine-Hugoniot condition for a stationary jump, but physical principles and many admissibility criteria (e.g. the viscosity-capillarity criterion in [15], see also [10]) indicate that this is *not* an admissible jump. Our numerical result shows the evolution of this jump into a more complicated structure of jumps, Figure 3a, apparently due to the inherent numerical viscosity of the scheme (see Remark 2.1). The solution exibits oscillatory behaviors near the phase boundary, Figure 3a. This is unpleasant but not surprising since we used component by component approximations in cells involving elliptic regions, hence during the process of one wave splitting into two or more waves, one or more of them being hyperbolic, oscillations occur as a failure of recognition of the corresponding characteristic fields. Similar oscillations

also appear for hyperbolic systems if a component by component approximation is used (see, e.g. [1]). The oscillations become smaller and more confined when the number of grids is increased (Figure 3b), indicating the convergence of the scheme even with these oscillations.

The background of Figure 3a is computed by the same scheme with 2000 points. It agrees with the result with 4000 points hence can be considered as a converged solution. In order to check whether this weak solution is admissible as a viscosity-capillarity limit, we plot in Figure 3c the numerical solutions of (1.4), for $A = \frac{1}{4}$, with $\epsilon = 0.1, 0.01, 0.001$ and the solution of our scheme for (1.2). The solutions to (1.4) are computed by the standard fourth order centered scheme with the classical fourth order Runge-Kutta time discretization. We verify adequate resolution for the solution of (1.4) for each fixed ϵ by repeatedly refining the mesh until the solutions do not change to visual inspection (the largest number of grid points used is 8000). Clearly we can see the convergence of the solutions of (1.4) to our solution when $\epsilon \to 0^+$ in Figure 3c.

(3) $(v_L, w_L) = (1, 0.45)$, $(v_R, w_R) = (2, 1.5)$. This case is somewhat easier to compute than the previous case, since the initial condition is not a steady nonadmissible weak solution. Figure 4a shows the result with 200 grid points on a background of a converged solution with 2000 grid points. Figure 4b shows the convergence as $\epsilon \to 0^+$ of the solutions of the viscosity-capillarity equation (1.4) to our solution.

We then compute the solutions for smooth initial conditions:

(1) $(v^0(x), w^0(x)) = (1 - 0.5cos(x), 1 + 0.5sin(x))$. This initial condition crosses the elliptic regions (Figure 5). The solution gradually evolves into piecewise smooth solutions contained entirely inside one of the two hyperbolic regions $w \leq \alpha$ and $w \geq \beta$, connected by jumps over the elliptic regions (phase transitions). This seems to agree with the physical intuition.

(2) $(v^0(x), w^0(x)) = (1 - 0.5cos(x), 0.8 + 0.2sin(x))$. This initial condition is entirely contained in the elliptic region. However, similar to the previous case, the solution gradually evolves into piecewise smooth solutions separated by phase transitions, Figure 6. Notice that during the evolution oscillations are generated inside the elliptic regions, presumably due to the inherent instability of the equation in those regions. These oscillations fade out once the solution evolves into the hyperbolic regions.

4 Concluding Remarks

Numerical methods for solving systems of conservation laws of mixed hyperbolic-elliptic type are investigated, through a flux splitting to write the physical elliptic flux as a sum

of two hyperbolic fluxes with positive/negative eigenvalues, then to apply the essentially non-oscillatory (ENO) high order finite difference methods on each of them. The method, in the simplest first order case, is equivalent to adding a numerical dissipation term with a diagonal dissipation matrix. The numerical results on the van der Waals equation of gas dynamics indicate that the method can resolve phase boundaries well and can be used as a tool to study the evolution of elliptic regions. More numerical tests on different mixed type equations constitute current research.

Acknowledgment: I am grateful to Haitao Fan and Din-Yu Hsieh for bringing my attention to the mixed type problems and for many helpful discussions.

References

[1] B. Cockburn, S.-Y. Lin and C.-W. Shu, *J. Comput. Phys.*, **84**, 90 (1989).

[2] H. Fan, *A limiting "viscosity" approach to the Riemann problem for the materials exhibiting change of phase (II), Arch. Rational Mech. Anal.*, to appear.

[3] H. Fan, *The existence, uniqueness and stability of solutions of the Riemann problem of systems of conservation laws of mixed type, (I) and (II)*, preprint.

[4] A. Harten, *J. Comput. Phys.*, **49**, 357 (1983).

[5] A. Harten and S. Osher,*SIAM J. Numer. Anal.*, **24**, 279 (1987).

[6] A. Harten, B. Engquist, S. Osher and S. Chakravarthy, *J. Comput. Phys.*, **71**, 231 (1987).

[7] D.-Y. Hsieh, *J. Math. Phys.*, **28**, 1589 (1987).

[8] R.D. James, *Arch. Rational Mech. Anal.*, **73**, 125 (1980).

[9] A. Rogerson and E. Meiburg, *A numerical study of the convergence properties of ENO schemes*, preprint, Submitted to *J. Sci. Comput.*

[10] M. Shearer, *Arch. Rational Mech. Anal.*, **93**, 45 (1986).

[11] M. Shearer, *Quarterly Appl. Math.*, **46**, 631 (1988).

[12] C.-W. Shu and S. Osher, *J. Comput. Phys.*, **77**, 439 (1988).

[13] C.-W. Shu and S. Osher, *J. Comput. Phys.*, **83**, 32 (1989).

[14] C.-W. Shu, *Numerical experiments on the accuracy of ENO and modified ENO schemes*, preprint, submitted to *J. Sci. Comput.*

[15] M. Slemrod, *Arch. Rational Mech. Anal.*, **81** 301,(1983).

[16] M. Slemrod, *Arch. Rational Mech. Anal.*, **105**, 327, (1989).

[17] A. Sommerfeld, *Thermodynamics and statistical mechanics* (Academic Press, New York and London, 1964).

[18] G. Strang, *SIAM J. Numer. Anal.*, **5**, 506 (1968).

[19] B. van Leer, *J. Comput. Phys.*, **32**, 101, (1979).

Figure 1: $p(w) = \frac{1}{w-0.25} - \frac{0.9}{w^2}$.

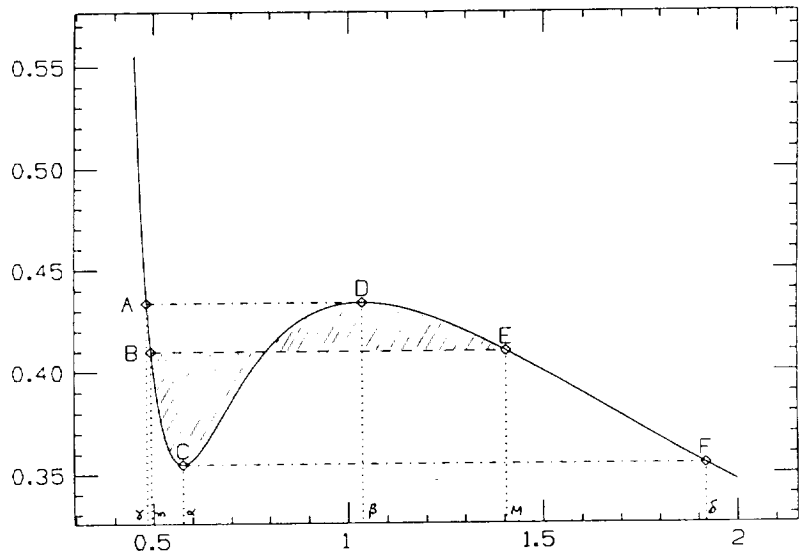

Figure 2: Maxwell solution, $(v_L, w_L) = (1, m)$, $(v_R, w_R) = (1, M)$, t=25. 200 points (plus) and the exact solution (solid line). Here and in what follows, the region between the two dashed lines is elliptic.

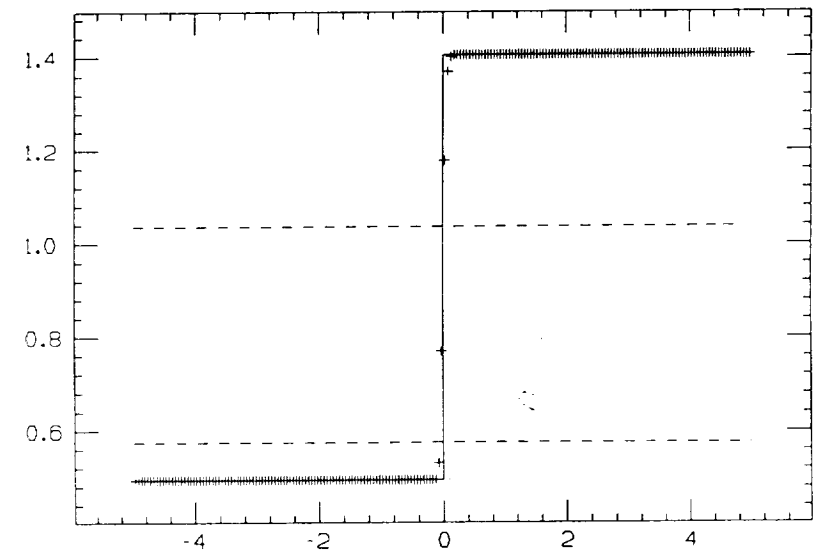

Figure 3: $(v_L, w_L) = (1, 0.54)$, $(v_R, w_R) = (1, 0.54)$, t=4. 3a: 200 points (plus) and 2000 points (solid line); 3b: 2000 points; 3c: centered solutions of (1.4) with $\epsilon = 0.1, 0.01, 0.001$, and ENO solution for (1.2).

Figure 3a

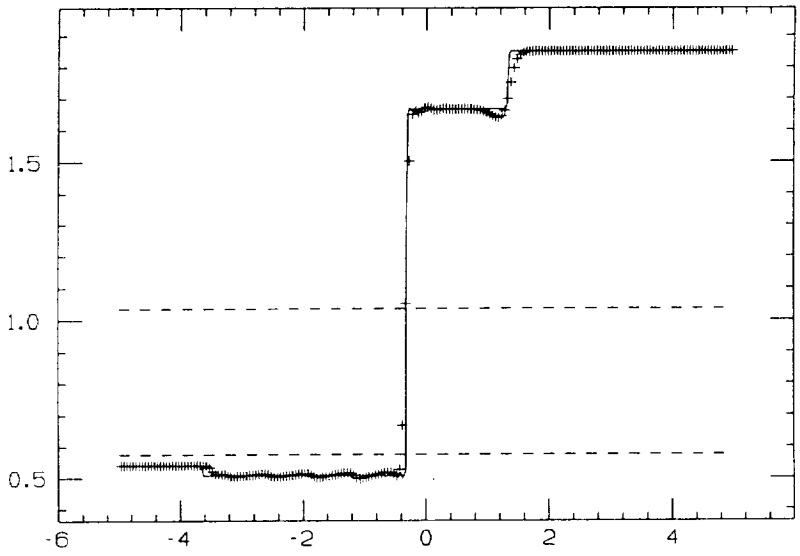

Figure 3b

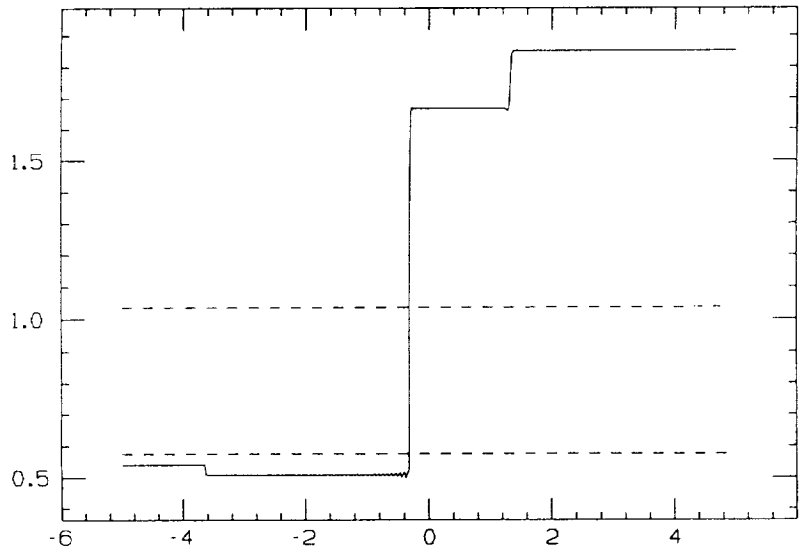

Figure 3c

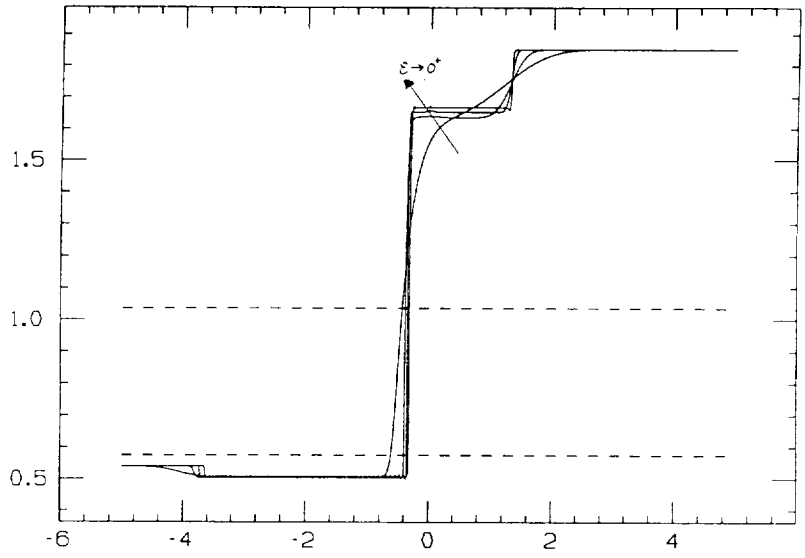

Figure 4: $(v_L, w_L) = (1, 0.45)$, $(v_R, w_R) = (2, 1.5)$, t=1.5. 4a: 200 points (plus) and 2000 points (solid line); 4b: centered solutions of (1.4) with $\epsilon = 0.1, 0.01, 0.001$, and ENO solution for (1.2).

Figure 4a

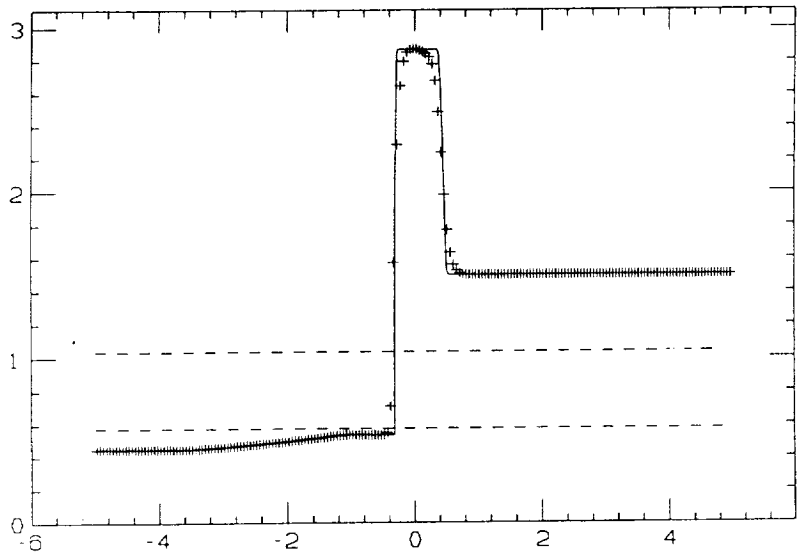

Figure 4b

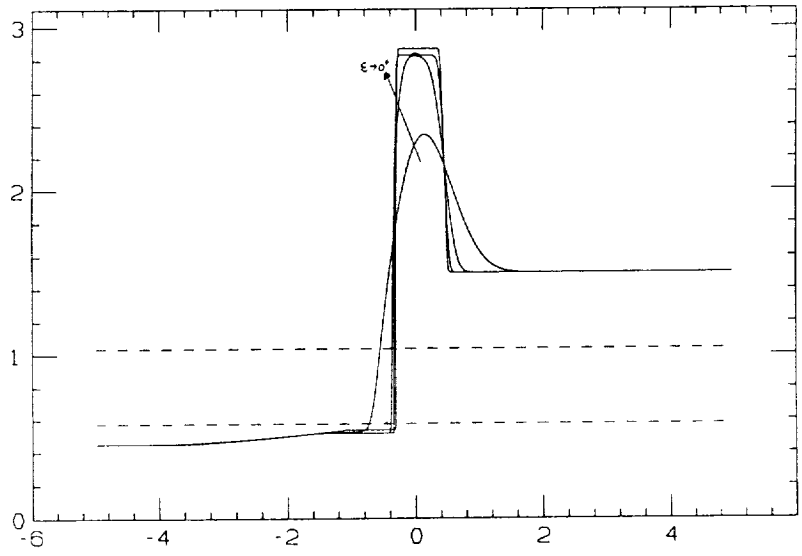

Figure 5: $(v^0(x), w^0(x)) = (1 - 0.5cos(x), 1 + 0.5sin(x))$. 400 grid points. t=0, .2, .4, .6, .8, 1, 1.2, 1.4, 1.6, 1.8, 2.

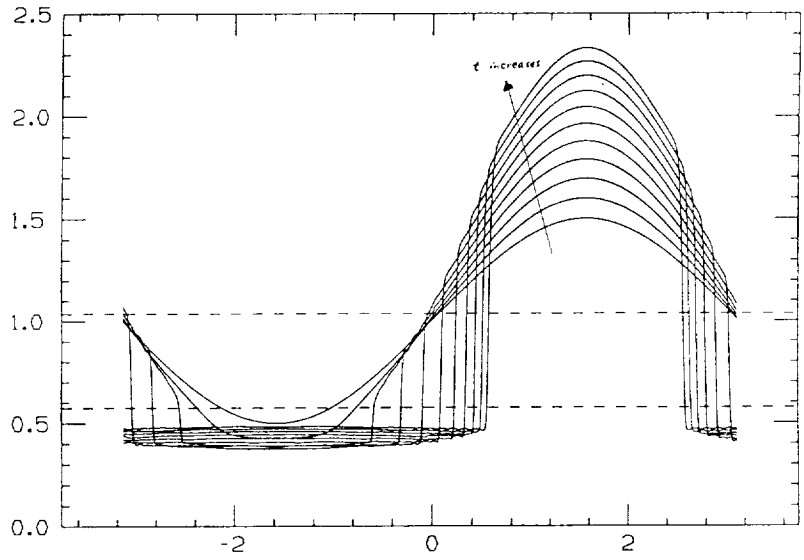

Figure 6: $(v^0(x), w^0(x)) = (1 - 0.5cos(x), 0.8 + 0.2sin(x))$. 400 grid points. t=0, .2, .4, .6, .8, 1, 1.2, 1.4, 1.6, 1.8, 2.

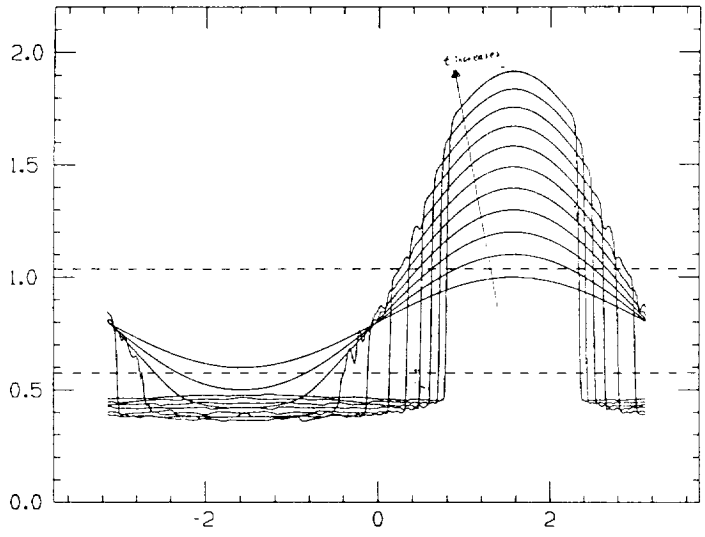

NASA National Aeronautics and Space Administration

Report Documentation Page

1. Report No.	2. Government Accession No.	3. Recipient's Catalog No.
NASA CR-182084 ICASE Report No. 90-56		

4. Title and Subtitle	5. Report Date
NUMERICAL METHODS FOR SYSTEMS OF CONSERVATION LAWS OF MIXED TYPE USING FLUX SPLITTING	August 1990
	6. Performing Organization Code
7. Author(s)	8. Performing Organization Report No.
Chi-Wang Shu	90-56
	10. Work Unit No.
9. Performing Organization Name and Address	505-90-21-01
Institute for Computer Applications in Science and Engineering Mail Stop 132C, NASA Langley Research Center Hampton, VA 23665-5225	11. Contract or Grant No. NAS1-18605
12. Sponsoring Agency Name and Address	13. Type of Report and Period Covered
National Aeronautics and Space Administration Langley Research Center Hampton, VA 23665-5225	Contractor Report
	14. Sponsoring Agency Code

15. Supplementary Notes

Langley Technical Monitor:
Richard W. Barnwell

Submitted to Journal of Computational Physics

Final Report

16. Abstract

The essentially non-oscillatory (ENO) finite difference scheme is applied to systems of conservation laws $\mathbf{u}_t + \mathbf{f}(\mathbf{u})_x = 0$ of mixed hyperbolic-elliptic type. A flux splitting $\mathbf{f}(\mathbf{u}) = \mathbf{f}^+(\mathbf{u}) + \mathbf{f}^-(\mathbf{u})$, with the corresponding Jacobi matrices $\frac{\partial \mathbf{f}^{\pm}(\mathbf{u})}{\partial \mathbf{u}}$ having real and positive/negative eigenvalues, is used. The hyperbolic ENO operator is applied separately on $\mathbf{f}^+(\mathbf{u})_x$ and on $\mathbf{f}^-(\mathbf{u})_x$. The scheme is numerically tested on the van der Waals equation in fluid dynamics. We observe convergence with good resolution to weak solutions for various Riemann problems, which are then numerically checked to be admissible as the viscosity-capillarity limits. We also observe the interesting phenomena of the shrinking of elliptic regions if they are present in the initial conditions.

17. Key Words (Suggested by Author(s))	18. Distribution Statement
ENO schemes, conservation laws, mixed type, van der Waals equation	64 - Numerical Analysis Unclassified - Unlimited

19. Security Classif. (of this report)	20. Security Classif. (of this page)	21. No. of pages	22. Price
Unclassified	Unclassified	17	A03